HTML ABSTRACT + LINKS

Calculations and measurements of x-ray Thomson scattering spectra in warm dense matter

G. Gregori*, S. H. Glenzer*, R. W. Lee*, D. G. Hicks*, J. Pasley†, G. W. Collins*, P. Celliers*, M. Bastea*, J. Eggert*, S. M. Pollaine* and O. L. Landen*

*Lawrence Livermore National Laboratory, PO Box 5508, Livermore, CA 94551
†Imperial College, University of London, Prince Consort Rd., London, England

Abstract. We present analytical expressions for the dynamic structure factor, or form factor $S(k,\omega)$, which is the quantity describing the inelastic x-ray cross section from a dense plasma or a simple liquid. Our results, based on the random phase approximation (RPA) for the treatment on the charged particle coupling, can be applied to describe scattering from either weakly coupled classical plasmas or degenerate electron liquids. Our form factor correctly reproduces the Compton energy downshift and the usual Fermi-Dirac electron velocity distribution for $S(k,\omega)$ in the case of a cold degenerate plasma. The results shown in this work can be applied to interpreting x-ray scattering in warm dense plasmas occurring in inertial confinement fusion experiments. We show that electron density, electron temperature and ionization state can be directly inferred from such measurements. Specifically, we present as an example, use the results of experiments performed at the Vulcan laser facility at the Rutherford Appleton Laboratories (UK) on a LiH target.

1. INTRODUCTION

Diagnostics of dense plasmas poses several difficulties as currently adopted experimental techniques are rather limited in probing particle densities, temperatures and charge states of warm dense matter. Optical techniques, for example, can only provide information on surface layers of dense plasmas since they are opaque to visible or UV light. On the other hand, the emerging interest in understanding the properties of matter under extreme conditions, as the ones achieved in inertial confinement fusion (ICF) experiments [1], necessitates the developing of finite temperature dense matter probes. In ICF implosion experiments a variety of plasma regimes are created, and of particular interest are Fermi degenerate (or quantum) plasmas, characterized by a Fermi temperature greater than the electron kinetic temperature. Moreover, equation of state (EOS) predictions for various degenerate plasmas can only be resolved by accurate measurements of the chemical state of the materials. However, uncertainties in the present data and the lack of reliable independent measurements of temperature and density have made the validation of current models and calculations difficult.

We investigate the possibility of extending spectrally resolved Thomson scattering [2] in the x-ray regime for the diagnostics of solid density plasmas. This method was first discussed by Landen *et al.* [3] as a viable diagnostics alternative in ICF experiments. In

CP645, *Spectral Line Shapes: Volume 12, 16th ICSLS*, edited by C. A. Back
© 2002 American Institute of Physics 0-7354-0100-4/02/$19.00

Downloaded 01 Feb 2008 to 128.115.27.10. Redistribution subject to AIP license or copyright; see http://proceedings.aip.org/proceedings/cpcr.jsp

Ref. [3], calculations were presented for scattering parameters $\alpha = 1/k\lambda_D \ll 1$, where λ_D is the Debye length and $\mathbf{k} = \mathbf{k}_0 - \mathbf{k}_1$ is the difference between the wave-number of the scattered and the incident probe radiation. In the present work, we provide a theoretical expression for the scattering form factor to represent x-ray Thomson scattering for arbitrary α parameter. In addition, our treatment can be applied in the description of scattering from degenerate to weakly coupled plasmas. For plasmas obeying the classical statistics, the electron-electron coupling constant is defined as (see, *e.g.,* Ichimaru [4]) $\Gamma = e^2/4\pi\varepsilon_0 k_B T_e d$, where T_e is the electron temperature and $d = (3/4\pi n_e)^{1/3}$ the ion-sphere radius, with n_e the electron density. In other words, Γ is the ratio between the potential and the kinetic energy of the electrons. For coupling between different charged particles, we also need to account for the ionization state of the material.

In an ideal plasma, $\Gamma \ll 1$ and the kinetic energy dominates the particle motion with negligible inter-particle coupling, while in a strongly coupled plasma, $\Gamma \gg 1$, the electrostatic (Coulomb) forces determine the nature of the particle motion. Weakly coupled plasmas lie in the range $\Gamma \lesssim 1$. The extension of definition of the coupling constant Γ to the quantum domain (*i.e.,* a degenerate plasma) is discussed by Liboff [5]. In this case, quantum diffraction prevents the electrons to get arbitrarily close to each other and Γ is now the ratio between the potential and the Fermi energy, E_F, of the electrons. Having $E_F = \hbar^2(3\pi^2 n_e)^{2/3}/2m_e$, as electron density increases, in contrast to a classical plasma, the coupling constant decreases, since $\Gamma \equiv \Gamma_q = e^2/4\pi\varepsilon_0 E_F d \sim n_e^{-1/3}$.

2. THEORY

2.1. Basic definitions

We are interested in describing the scattering from a uniform plasma containing N ions per unit volume. If Z_A is the nuclear charge of the ion, the total number of electrons per unit volume in the system, including free and bound ones, is $Z_A N$. Let us now assume we probe such a system with x-rays of frequency ω_0 such that $\hbar\omega_0 \gg E_I$, with E_I the ionization energy of any bound electron, *i.e.,* the incident frequency must be large compared to any natural absorption frequency of the scattering atom, which allows us to neglect photoabsorption. During the scattering process, the incident photon transfers momentum $\hbar\mathbf{k}$ and energy $\hbar\omega = \hbar^2 k^2/2m_e = \hbar\omega_0 - \hbar\omega_1$ to the electron, where ω_1 is the frequency of the scattered radiation. Under these conditions we can distinguish between electrons that are *kinematically* free with respect to the scattering process and *core* electrons that are tightly bound to the atom. If a_n is the orbital radius of the electron with principal quantum number n, kinematically free electrons satisfy the relation [6, 7] $ka_n \gtrsim 1$ (in the hydrogenic approximation, $a_n \sim a_B n^2/Z_A$ with $a_B = 4\pi\varepsilon_0\hbar^2/m_e e^2$ the Bohr radius), while the opposite inequality applies for core electrons. This condition is equivalent to assuming that $\hbar\omega$, the energy transferred to the electron by Compton scattering, is larger than its binding energy. In the non-relativistic limit ($\hbar\omega \ll \hbar\omega_0$)

$$k = |\mathbf{k}| = \frac{4\pi}{\lambda_0}\sin(\theta/2), \tag{1}$$

Downloaded 01 Feb 2008 to 128.115.27.10. Redistribution subject to AIP license or copyright; see http://proceedings.aip.org/proceedings/cpcr.jsp

with λ_0 the probe wavelength and θ the scattering angle. We denote with Z_f and Z_c the number of kinematically free and core electrons, respectively. Clearly, $Z_A = Z_f + Z_c$. To avoid possible confusions, we should stress that Z_f is conceptually different from the *true* ionization state of the atom. It includes both the truly free (removed from the atom by ionization) and the valence (weakly bound) electrons; thus $Z_f = Z + Z_v$, where Z is the number of electrons removed from the atom, and Z_v is the number of valence electrons. In the limiting case of a liquid metal, $Z = 0$, and only the valence (or conduction) electrons need to be considered.

2.2. Scattering cross section

Following the approach of Chihara [8, 9] the scattering cross section is described in terms of the dynamic structure factor of all the electrons in the plasma

$$\frac{d^2\sigma}{d\Omega d\omega} = \sigma_T \frac{k_1}{k_0} S(k,\omega), \tag{2}$$

where σ_T is the usual Thomson cross section and $S(k,\omega)$ is the total dynamic structure factor defined as

$$S(k,\omega) = \frac{1}{2\pi}\int e^{i\omega t}\langle \rho_e(\mathbf{k},t)\rho_e(-\mathbf{k},0)\rangle dt, \tag{3}$$

with $\langle ... \rangle$ denoting a thermal average and

$$\rho_e(\mathbf{k},t) = \sum_{s=1}^{Z_A N} \exp[i\mathbf{k}\cdot\mathbf{r}_s(t)], \tag{4}$$

is the Fourier transform of the total electron density distribution, with $\mathbf{r}_s(t)$ the time dependent position vector of the s-th electron. Assuming the system is isotropic, as in the case of interest here (liquid metals or plasmas), the dynamic structure factor depends only on the magnitude of k, not on its direction. The next step consists in separating the total density fluctuation, Eq. (4), between the free (Z_f) and core (Z_c) electron contributions, and separating the motion of the electrons from the motion of the ions. The details of procedure are given by Chihara [8, 9], thus obtaining for the dynamic structure:

$$S(k,\omega) = |f_I(k) + q(k)|^2 S_{ii}(k,\omega) + Z_f S^0_{ee}(k,\omega) + Z_c \int \tilde{S}_{ce}(k,\omega-\omega')S_s(k,\omega')d\omega'. \tag{5}$$

The first term in Eq. (5) accounts for the density correlations of electrons that dynamically follow the ion motion. This includes both the core electrons, represented by the ion form factor $f_I(k)$, and the screening cloud of free (and valence) electrons that surround the ion, represented by $q(k)$ [10]. $S_{ii}(k,\omega)$ is the ion-ion density correlation function. The second term in Eq. (5) gives the contribution in the scattering from the free electrons that do not follow the ion motion. Here, $S^0_{ee}(k,\omega)$ is the high frequency part of the electron-electron correlation function [11] and it reduces to the usual electron feature

Downloaded 01 Feb 2008 to 128.115.27.10. Redistribution subject to AIP license or copyright; see http://proceedings.aip.org/proceedings/cpcr.jsp

[12, 13] in the case of an optical probe. Inelastic scattering by core electrons is included in the last term of Eq. (5), which arises from Raman transitions to the continuum of core electrons within an ion, $\tilde{S}_{ce}(k,\omega)$, modulated by the self-motion of the ions, represented by $S_s(k,\omega)$. We point out that in Eq. (5) electron-ion correlations are implicitly accounted in the first term, since, as shown by Chihara [8], the electron-ion response function can be written in terms of the ion-ion response function. We observe that the total density correlation function must obey the relation [14]

$$S(k,-\omega) = \exp(-\hbar\omega/k_B T_e) S(k,\omega), \tag{6}$$

which is a consequence of detail balance. This gives rise to asymmetry in the spectrum as we will discuss further in the next sections.

The ion-ion correlations reflect the thermal motion of the ions and/or the ion plasma frequency, and since we cannot currently experimentally access this low frequency part of the spectrum, we can approximate $S_{ii}(k,\omega) = S_{ii}(k)\delta(\omega)$. We thus only need to calculate the static structure factor for ion-ion correlations. We shall also observe that for typical conditions in dense plasmas for ICF experiments, the ions are always non-degenerate, since their thermal de Broglie wavelength is much smaller than the average interparticle distance. On the other hand, the electrons can exhibit some degree of degeneracy, and in the case of very cold and dense plasmas, they will obey the Fermi-Dirac distribution. Under these conditions, and within the framework of the random phase approximation (RPA), we can calculate $S_{ii}(k)$ using the semi-classical approach suggested by Arkhipov and Davletov [15], which is based on a pseudo-potential model for the interaction between charged particles to account for quantum diffraction effects (*i.e.*, the Pauli exclusion principle) and symmetry [16]. The correlation function is then calculated at the effective temperature $T_{cf} \sim (T_e^2 + T_q^2)^{1/2}$, where $T_q = T_F/(1.3251 - 0.1779\sqrt{r_s})$, with $r_s = d/a_B$. From quantum Monte Carlo calculations this corrected temperature was shown [17] to reproduce the exact quantum statistics at kinetic temperatures well below the Fermi temperature ($T_e \ll T_F$).

The free electron density-density correlation function that appears in the second term of Eq. (5) can be formally obtained through the fluctuation-dissipation theorem [18]:

$$S_{ee}^0(k,\omega) = -\frac{\hbar}{1-\exp(-\hbar\omega/k_B T_e)} \frac{\varepsilon_0 k^2}{\pi e^2 n_e} \mathrm{Im}\left[\frac{1}{\varepsilon(k,\omega)}\right], \tag{7}$$

where $\varepsilon(k,\omega)$ is the electron dielectric response function. In the case of an ideal classical plasma, the plasma dielectric response is evaluated from a perturbation expansion of the Vlasov equation [19]. The resultant form for the density correlation function is then known as the Salpeter electron feature [12]. This approach, however, fails when the electrons become degenerate or nearly degenerate as quantum effects begin to dominate. Under the assumption that interparticle interactions are weak, so that the nonlinear interaction between different density fluctuations is negligible, the dielectric function can be derived in the random phase approximation (RPA) [20, 21]. In the classical limit, it reduces to the usual Vlasov equation.

We shall stress the point that in the limit of the RPA, strong coupling effects are not accounted for, thus limiting the model validity to plasma conditions in the range $\Gamma \sim 1$.

Downloaded 01 Feb 2008 to 128.115.27.10. Redistribution subject to AIP license or copyright; see http://proceedings.aip.org/proceedings/cpcr.jsp

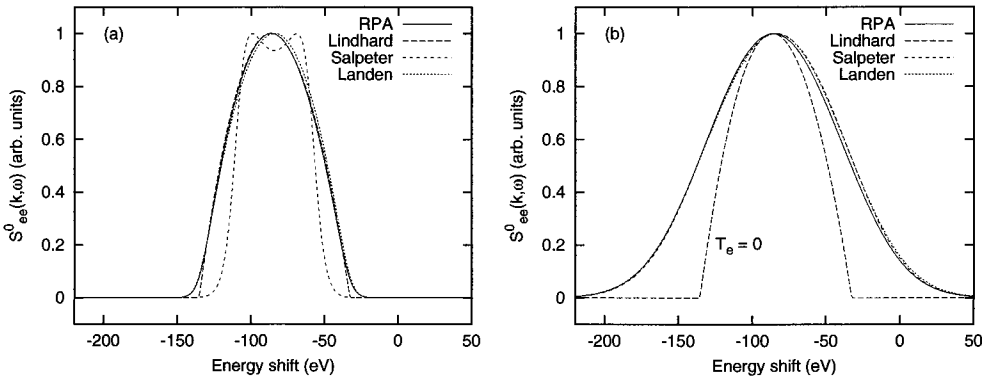

FIGURE 1. Free electron dynamic structure $S^0_{ee}(k,\omega)$ for $n_e = 1.0 \times 10^{23}$ cm^{-3} at $T_e = 1$ eV (a) and $T_e = 10$ eV (b). The probe radiation is $\lambda_0 = 0.26$ nm and the scattering angle is $\theta = 160^o$, and $\alpha = 0.40$ (a) or $\alpha = 0.29$ (b).

Use of the RPA at larger couplings may still provide fairly accurate results if $kd \gtrsim 1$ [22, 23]. In the cases studied here, the plasma are within the range of validity. However, extensions to strong coupling are possible in terms of a local field correction [24] of the dielectric response functions, but they are significantly more complex and can be obtained only through the solution of the hypernetted chain (HNC) equation [25] or molecular dynamics simulations [26].

In Fig. 1 we have plotted normalized line profiles of $S^0_{ee}(k,\omega)$ calculated assuming incident x-rays with $\lambda_0 = 0.26$ nm, corresponding to the Ti He-α 4.75 keV emission line, and a scattering angle of $\theta = 160^o$. The various models compared with the RPA in Fig. 1 are the analytical Lindhard-Sommerfeld theory [21], which is exact for $T_e = 0$ eV, the classical Salpeter form factor, and the calculations of Landen *et al.* [3] which is a direct representation of the electron distribution function. We observe that the RPA calculation automatically includes the effect of the Compton energy downshift in the scattered spectrum. This is not true, for example, in the Salpeter and Landen approximations since momentum transfer from the photons to the electrons is neglected there. Thus, in order to compare with the RPA, we need to translate the entire line profile an amount that corresponds to a shift of $\hbar^2 k^2/2m_e$ in energy. At a density of $n_e = 1.0 \times 10^{23}$ cm^{-3}, the Fermi temperature is $T_F = 7.85$ eV. We indeed see that, at temperatures lower than T_F, when quantum effects are important, the Salpeter result deviates from the RPA one. On the other hand, at $T_e = 10$ eV ($T_e > T_F$), the Salpeter formula agrees very well with the RPA since now the kinetic temperature is comparable with T_F. From Fig. 1 we also see that at $T_e = 1$ eV the calculated profile of $S^0_{ee}(k,\omega)$ is parabolic, while at $T_e = 10$ eV the profile is Gaussian. The transition from a parabolic to a Gaussian profile, as the electron temperature is raised, corresponds to the transition from Fermi to Boltzmann statistics in the electron velocity distribution.

It is customary to describe scattering processes in terms of the parameter $\alpha = 1/ks$, where s is the characteristic screening length of the electrostatic interactions. For a

Downloaded 01 Feb 2008 to 128.115.27.10. Redistribution subject to AIP license or copyright; see http://proceedings.aip.org/proceedings/cpcr.jsp

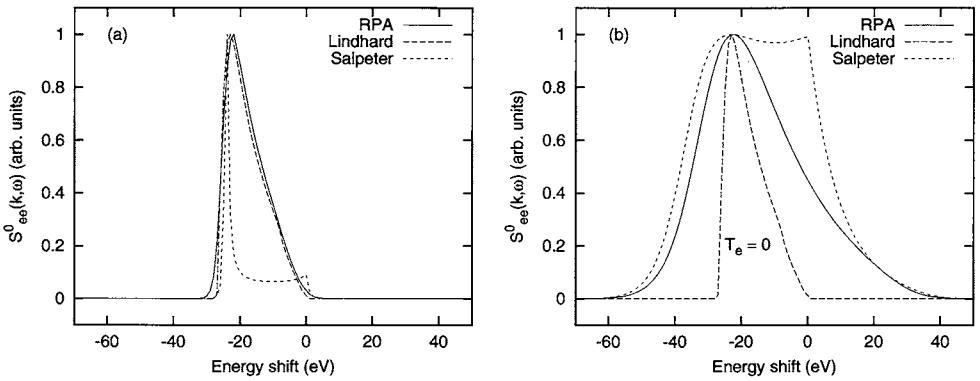

FIGURE 2. Free electron dynamic structure $S^0_{ee}(k,\omega)$ for $n_e = 1.0 \times 10^{23}$ cm^{-3} at $T_e = 1$ eV (a) and $T_e = 10$ eV (b). The probe radiation is $\lambda_0 = 0.78$ nm and the scattering angle is $\theta = 160^o$, and $\alpha = 1.17$ (a) or $\alpha = 0.85$ (b).

classical plasma s coincides with the Debye length λ_D. If $\alpha < 1$ the electrons behave as uncorrelated scatters, while for large α parameters the scattering reflects their collective motion. In a classical plasma $\alpha \sim (T_e/n_e)^{1/2}$, and the nature of the scattering depends on both the electron temperature and the electron density. As the plasma becomes degenerate, the Debye length does not represent anymore the screening of the Coulomb forces. However, the classical results are still valid if, instead of using the kinetic temperature, they are evaluated at the effective temperature T_{cf} [17]. Fig. 4 shows $\alpha = const$ contours in the T_e-n_e plane for typical experimental conditions. We see that in the case of an ideal ($r_s \to 0$) degenerate electron liquid this approximation yields $s \sim \lambda_{TF}$, where $\lambda_{TF} = \sqrt{2\varepsilon_0 E_F/3n_e e^2}$ is the Thomas-Fermi screening length. Thus, $\alpha \sim n_e^{-1/6}$ and the type of scattering (uncorrelated or collective) is independent of T_e and weakly dependent on the electron density. The collective nature of the scattering can thus be investigated by only changing the wavelength of the probe x-ray.

Dynamic structures for collective scattering (*i.e.,* large α parameters) are shown in Fig. 2, which correspond to a longer probe radiation of wavelength $\lambda_0 = 0.78$ nm (Al He-α 1.6 keV emission line), all the other conditions being the same as in Fig. 1. In both Figs. 1 and 2 we see the strong asymmetry in the line profiles resulting from the detail balance relation (6).

The last term in Eq. (5) corresponds to the density correlations of the tightly bound electrons within each single ion, and it arises from electron-hole and bound excitations of the inner core electrons. The Fermi *golden rule* in the first order perturbation theory can be used to calculate the spectrum resulting from electron-hole excitations [27, 28]. As discussed by Mizuno and Omura [7] inner core electrons can be excited by the probe radiation to continuum states and the corresponding spectrum of the scattered radiation is that of a Raman-type band. Since the Raman band has width comparable or larger than the Compton band [29], we can regard this type of contribution as yielding only a small background [27]. This seems consistent with the results presented by Glenzer [30]

Downloaded 01 Feb 2008 to 128.115.27.10. Redistribution subject to AIP license or copyright; see http://proceedings.aip.org/proceedings/cpcr.jsp

on x-ray scattering from moderately heated beryllium targets.

3. THOMSON SCATTERING PROFILES: COMPARISON WITH EXPERIMENTS

Based on the theory outlined in the previous sections, we are now able to calculate the full Thomson scattering profile for x-ray probes at arbitrary scattering angle, for either classical or quantum plasmas. The only limitation is that the degree of coupling must not be too large to invalidate the limits of the RPA. We have obtained synthetic line profiles for the Ti He-α 4.75 keV radiation probe at $\theta = 160^{\circ}$ scattering angle. In addition, we have assumed that the probe material consists of LiH ($Z_A = 4$) at $T_e = 1$ eV and at various compressed densities. To simulate actual experimental data, the theoretical line profile from Eq. (5) has been convoluted with a Gaussian instrument function with 40 eV FWHM. From Fig. 3 we can see that synthetic line profiles tend to be fairly similar since the broadening of the Compton profile goes as $\sqrt{T_F} \sim n_e^{1/3}$. The effect of the ionization state on the line profiles can also be seen in Fig. 3. Here, we have plotted synthetic lineshapes for different values of Z_f (or Z_c) with $n_e = 1.0 \times 10^{23}$ cm^{-3} ($T_F = 7.85$ eV) and $T_e = 1$ eV or $T_e = 10$ eV. We see dramatic differences in the simulated lineshapes for the various Z_f. This effect then suggests that x-ray Thomson scattering can also be implemented as a diagnostics tool for the ionization state of solid density plasmas based on the difference in the intensity between the unshifted and the Compton shifted peaks. This possibility was suggested by Landen *et al.* [3] since current optical techniques cannot directly measure the number of free electrons in solid density plasmas, and it extends the ionization state measurements based on visible light Thomson scattering [31]. On the other hand, the ratio of the scattered intensities between the shifted and the unshifted peaks is only sensitive to Z_f which is *not* the same as Z, the true ionization state of the material. The measure of Z_f will thus only provide an upper bound to Z, unless the number of valence electrons can be calculated or determined by other techniques.

Preliminary data obtained from a LiH target, with initial density of 0.77 g/cc, probed at the Vulcan laser facility at the Rutherford Appleton Laboratory with Ti He-α 4.75 keV x-rays have been compared with our theoretical model. The initial ion density is thus $n_i^0 = 5.8 \times 10^{22}$ cm^{-3}. The LiH target has been shocked and heated with two beams with approximate energy of 50 J/beam at 2ω, and 1 ns pulsewidth. X-ray line radiation has been generated by the interaction of a 110 J, 0.6 ns pulsewidth, 2ω laser beam on a Ti foil. The probe beam has been delayed 0.8 ns with respect to the heater beams. By shielding the view of the LiH target with 50 μm thick Au foils, a scattering angle of 160° can be selected. The scattering data have been collected using a mosaic HOPG (graphite) crystal used in focus mode in order to achieve high resolution and efficiency. The crystal was positioned 7.5 cm from the LiH target and the data were collected on an x-ray CCD camera 15 cm from the target. Comparison between the experimental line profile and the theoretical ones, convoluted with an instrument function of 30 eV FWHM, are shown in Fig. 4. We have $n_e \simeq 1.8 \pm 0.6 \times 10^{23}$ cm^{-3} ($T_F = 12.5$ eV) and $T_e \simeq$ 0-5 eV, with $Z_f = 3.2 \pm 0.1$. From Fig. 4, we see that typical error in the density fit is of the order of 30%, which is to be expected for preliminary quality data. These values corresponds to

Downloaded 01 Feb 2008 to 128.115.27.10. Redistribution subject to AIP license or copyright; see http://proceedings.aip.org/proceedings/cpcr.jsp

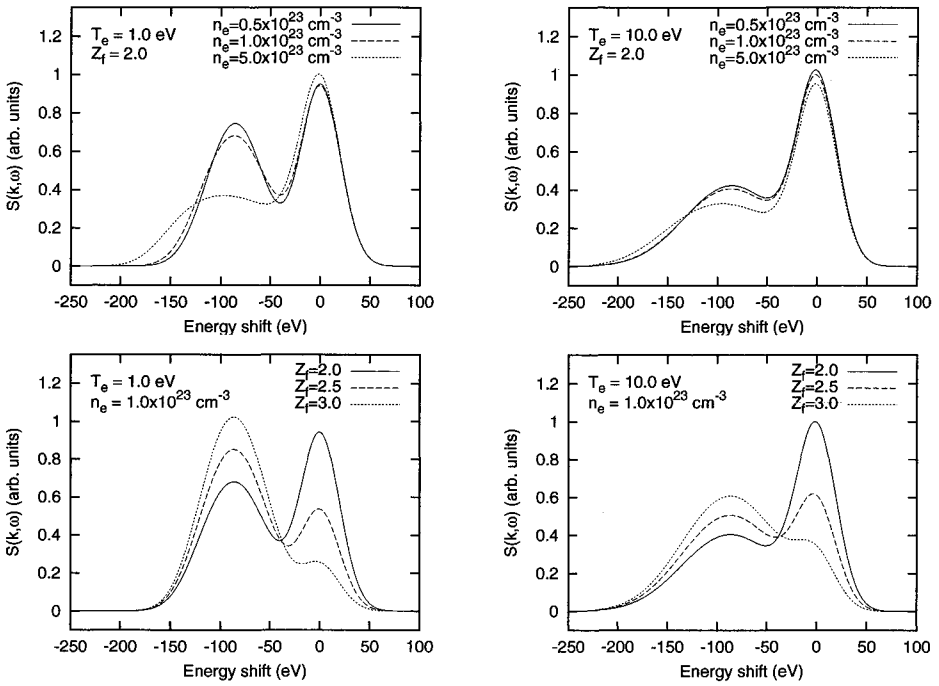

FIGURE 3. Synthetic dynamic structure $S(k,\omega)$ calculated for LiH target ($Z_A = 4$) at $T_e = 1$ eV and $T_e = 10$ eV. The probe radiation is $\lambda_0 = 0.26$ nm and scattering angle $\theta = 160^o$.

a compression ratio $\chi = n_e/Z_f n_i^0 \sim 0.6$-1.4. The theory reproduces sufficiently well the measured profile, suggesting that the analysis reported here may be fairly adequate in describing the scattering process. Also, measurement of the number of free (and bound) electrons can be performed directly from the experimental data. The temperature-density domain of interest for typical experimental conditions is also shown in Fig. 4. From the fitting results, we see that the Vulcan experiment lies on the line where the α parameter changes its slope, which corresponds, as we have previously discussed, to a change from the classical Debye screening to the Thomas-Fermi screening.

4. SUMMARY AND CONCLUDING REMARKS

In this paper we have presented analytical expressions for the inelastic x-ray form factor that can be easily applied to interpreting scattering experiments in solid and super-solid density degenerate-to-hot plasmas. We have shown that x-ray Thomson scattering can be used as an effective diagnostic technique in plasmas produced under extreme conditions as the ones occurring in ICF experiments or to simulate scattering conditions found in the interiors of planets. This new technique will be useful, for example, to directly

Downloaded 01 Feb 2008 to 128.115.27.10. Redistribution subject to AIP license or copyright; see http://proceedings.aip.org/proceedings/cpcr.jsp

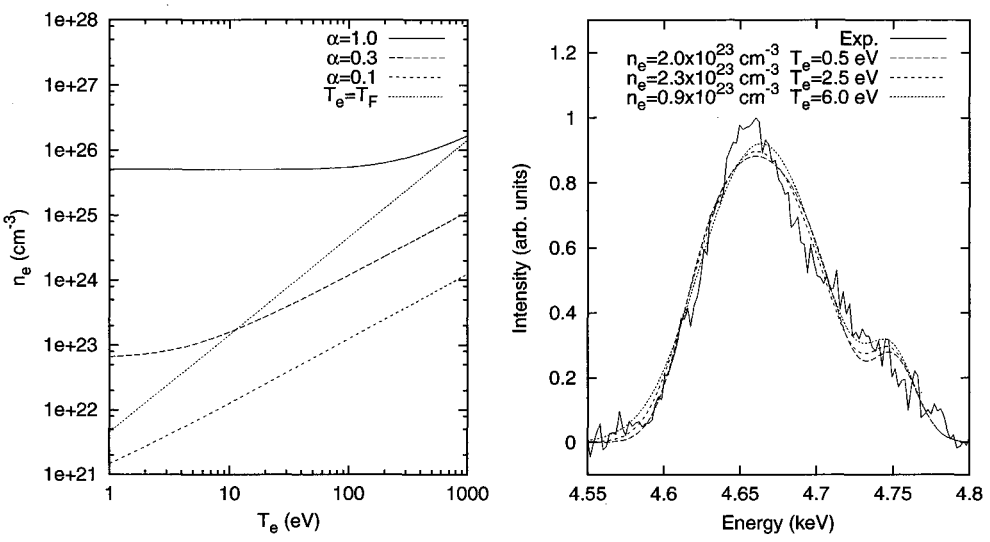

FIGURE 4. Left: calculated $\alpha = const$ contours for $\lambda_0 = 0.26$ nm and $\theta = 160^o$. The line $T_e = T_F$ is also plotted in figure. Right: preliminary experimental scattering profile from LiH target obtained with a probe radiation $\lambda_0 = 0.26$ nm and at a scattering angle of $\theta = 160^o$. Fitting parameters are given in the figure.

measure the electron temperature, ionization state or electron conductivity for EOS model validation.

Preliminary comparison with experiments conducted at the Vulcan laser facility on LiH targets have showns fair agreement between the model discussed in this paper and the experimental data, suggesting that x-ray Thomson scattering can be implemented as a viable diagnostics for low Z solid density plasmas.

ACKNOWLEDGMENTS

This work was performed under the auspices of the U.S. Department of Energy by the University of California Lawrence Livermore National Laboratory under Contract No. W-7405-ENG-48. We also acknowledge support from Laboratory Directed Research and Development grant No. 02-ERD-13.

REFERENCES

1. Lindl, J. D., *Inertial Confinement Fusion*, Springer-Verlag, New York, 1998.
2. Glenzer, S. H., Alley, W. E., Estabrook, K. G., de Groot, J. S., Haines, M. G., Hammer, J. H., Jadaud, J.-P., MacGowan, B. J., Moody, J. D., Rozmus, W., Suter, L. J., Weiland, T. L., and Williams, E. A., *Phys. Rev. Lett.*, **82**, 97 (1999).

Downloaded 01 Feb 2008 to 128.115.27.10. Redistribution subject to AIP license or copyright; see http://proceedings.aip.org/proceedings/cpcr.jsp

3. Landen, O. L., Glenzer, S. H., Edwards, M. J., Lee, R. W., Collins, G. W., Cauble, R. C., Hsing, W. W., and Hammel, B. A., *J. Quant. Spectrosc. Radiat. Transfer*, **71**, 465 (2001).
4. Ichimaru, S., *Rev. Mod. Phys.*, **54**, 1017 (1982).
5. Liboff, R. L., *J. Appl. Phys.*, **56**, 2530 (1984).
6. Bushuev, V. A., and Kuz'min, R. N., *Usp. Fiz. Nauk*, **122**, 81 (1977).
7. Mizuno, Y., and Ohmura, Y., *J. Phys. Soc. Japan.*, **22**, 445 (1967).
8. Chihara, J., *J. Phys. F: Met. Phys.*, **17**, 295 (1987).
9. Chihara, J., *J. Phys.: Condens. Matter*, **12**, 231 (2000).
10. Riley, D., Woolsey, N. C., McSherry, D., Weaver, I., Djaoui, A., and Nardi, E., *Phys. Rev. Lett.*, **84**, 1704 (2000).
11. Ichimaru, S., *Basic Principles of Plasma Physics*, Addison, Reading, MA, 1973.
12. Salpeter, E. E., *Phys. Rev.*, **120**, 1528 (1960).
13. Evans, D. E., and Katzenstein, J., *Rep. Prog. Phys.*, **32**, 207 (1969).
14. Hansen, J.-P., and McDonald, I. R., *Theory of Simple Liquids*, Academic, London, 2000.
15. Arkhipov, Y. V., and Davletov, A. E., *Phys. Lett. A*, **247**, 339 (1998).
16. Baus, M., and Hansen, J.-P., *Phys. Rep.*, **59**, 1 (1980).
17. Perrot, F., and Dharma-Wardana, M. W. C., *Phys. Rev. B*, **62**, 16536 (2000).
18. Kubo, R., *J. Phys. Soc. Japan*, **12**, 570 (1957).
19. Landau, L. D., Lifshitz, E. M., and Pitaevskii, L. P., *Physical Kinetics*, Pergamon, Oxford, 1995.
20. Pines, D., and Bohm, D., *Phys. Rev.*, **85**, 338 (1952).
21. Pines, D., and Nozieres, P., *The Theory of Quantum Fluids*, Addison-Wesley, Redwood, CA, 1990.
22. Cauble, R., and Boercker, D. B., *Phys. Rev. A*, **28**, 944 (1983).
23. Boercker, D. B., Lee, R. W., and Rogers, F. J., *J. Phys. B*, **16**, 3279 (1983).
24. Ichimaru, S., Mitake, S., Tanaka, S., and Yan, X.-Z., *Phys. Rev. A*, **32**, 1768 (1985).
25. Carley, D. D., *Phys. Rev.*, **131**, 1406 (1963).
26. Hansen, J.-P., "Molecular Dynamics Simulation of Coulomb Systems in two and three Dimensions," in *Molecular Dynamics Simulation of Statistical Mechanical Systems*, edited by G. Ciccotti and W. G. Hoover, North-Holland, Amsterdam, 1986, vol. 97.
27. Platzman, P. M., and Tzoar, N., *Phys. Rev.*, **139**, A410 (1965).
28. Eisenberger, P., and Platzman, P. M., *Phys. Rev. A*, **2**, 415 (1970).
29. Issolah, A., Garreau, Y., Levi, B., and Loupias, G., *Phys. Rev. B*, **44**, 11029 (1991).
30. Glenzer, S. H., *Bull. American Phys. Soc.*, **46**, 325 (2001).
31. Glenzer, S. H., Alley, W. E., Estabrook, K. G., de Groot, J. S., Haines, M. G., Hammer, J. H., Jadaud, J.-P., MacGowan, B. J., Moody, J. D., Rozmus, W., Suter, L. J., Weiland, T. L., and Williams, E. A., *Phys. Plasmas*, **6**, 2117 (1999).

Downloaded 01 Feb 2008 to 128.115.27.10. Redistribution subject to AIP license or copyright; see http://proceedings.aip.org/proceedings/cpcr.jsp